

**Space-borne  
observations link**

G. S. Jenkins and  
J.-H. Ryu

# Space-borne observations link the tropical Atlantic ozone maximum and paradox to lightning

**G. S. Jenkins and J.-H. Ryu**

Department of Meteorology, Penn State University, 503 Walker Building, University Park, Pennsylvania, USA

Received: 8 August 2003 – Accepted: 10 November 2003 – Published: 13 November 2003

Correspondence to: G. S. Jenkins (osei@essc.psu.edu)

Title Page

Abstract

Introduction

Conclusions

References

Tables

Figures

⏪

⏩

◀

▶

Back

Close

Full Screen / Esc

Print Version

Interactive Discussion

© EGU 2003

## Abstract

The causes of high tropospheric column ozone values over the Tropical Atlantic Ocean during September, October, and November (SON) are investigated by examining lightning during 1998–2001. The cause for high tropospheric column ozone in the hemisphere opposite of biomass burning (tropical ozone paradox) is also examined. Our results show that lightning is central to high tropospheric column ozone during SON and responsible for the tropical ozone paradox during December, January, and February (DJF) and June, July and August (JJA). During SON large numbers of flashes are observed in South America, Central and West Africa enriching the tropospheric column ozone over the Tropical Atlantic Ocean. During JJA the largest numbers of lightning flashes are observed in West Africa, enriching tropospheric column ozone to the north of 5° S in the absence biomass burning. During DJF, lightning is concentrated in South America and Central Africa enriching tropospheric column ozone south of the Equator in the absence of biomass burning.

## 1. Introduction

Fishman et al. (1991) identified trends in total tropospheric column ozone (TCO) over the Tropical Atlantic using the Total Ozone Mapping Spectrometer (TOMS). They found that the highest TCO values (tropical ozone maximum) were found in Northern Hemisphere (NH) autumn (SON) primarily over the Southern Tropical Atlantic Ocean and likely associated with biomass burning in South America and Southern Africa. This feature was also found during the Transport and Atmospheric Chemistry Near the Equator-Atlantic (TRACE-A) field experiment (Fishman et al., 1996; Thompson et al., 1996). The TRACE-A observations identified regions of biomass burning and other anthropogenic sources of ozone and ozone precursors, horizontal and vertical transports of ozone/ozone precursors, and limited observations examined the association of lightning with the production of  $\text{NO}_x$  and  $\text{O}_3$  (Jacob et al., 1996). Weller et al. (1996)

### Space-borne observations link

G. S. Jenkins and  
J.-H. Ryu

Title Page

Abstract

Introduction

Conclusions

References

Tables

Figures

⏪

⏩

◀

▶

Back

Close

Full Screen / Esc

Print Version

Interactive Discussion

suggests that stratospheric intrusions of O<sub>3</sub> may also be responsible for elevated ozone in the upper troposphere.

A feature of interest during the Northern Hemisphere (NH) winter season (DJF), is the relationship between tropospheric ozone and biomass burning. During DJF, biomass burning is confined to the Northern Hemisphere primarily in West Africa. The highest TCO values, however, are still found over the Southern Tropical Atlantic Ocean and denoted as the Tropical Ozone Paradox (Weller et al., 1996; Thompson et al., 2000; Martin et al., 2002; Edwards et al., 2003). In the Aerosols99 Ship campaign, Thompson et al. (2000) found the highest ozone mixing ratios in the lower troposphere downstream of biomass burning over the Northern Tropical Atlantic, but in the middle/upper troposphere over the Southern Tropical Atlantic due most likely to lightning. Edwards et al. (2003) have linked the higher TCO values of the South Tropical Atlantic to lightning from Southern Africa and South America.

Kim et al. (2001) suggest that TOMS can underestimate the tropospheric ozone column if high ozone mixing ratios are found in the lower troposphere. Martin et al. (2002) have suggested that satellite derived TCO values are underestimated by 3–5 DU over West Africa during the biomass burning season (DJF) because the highest ozone mixing ratios are confined to the lower troposphere. On the other hand, during the months of June through October, Martin et al. (2002) suggest that TOMS overestimates TCO values over Northern Africa when compared to the MOSAIC data.

The objectives of this paper are: (1) to re-examine the causes for the apparent Tropical Ozone Paradox using satellite derived TCO data for the periods 1979–1992 and 1998–2001. In particular we identify the anthropogenic (biomass burning) and natural sources (lightning) of ozone, upper levels winds and its relationship to the TCO values over the Tropical Atlantic Ocean. (2) To examine the potential causes of why satellite estimates of TCO values over northern Africa are elevated during JJA and if it is related to lightning. (3) To examine the relationship between the Tropical Atlantic Ozone Maximum during SON and lightning over Africa and South America. Sinks of ozone such as photolysis, deposition and chemical transformation are not explored and

**Space-borne observations link**

G. S. Jenkins and  
J.-H. Ryu

Title Page

Abstract

Introduction

Conclusions

References

Tables

Figures

◀

▶

◀

▶

Back

Close

Full Screen / Esc

Print Version

Interactive Discussion

troposphere-stratosphere exchanges of air are also not considered.

## 2. Data description

The NCEP reanalysis (Kalnay et al., 1996) are used for wind at a horizontal resolution of  $2.5^{\circ} \times 2.5^{\circ}$ . The ozone data is the Tropical Tropospheric Ozone (TTO) data from the TOMS satellites produced at a horizontal resolution of  $1^{\circ} \times 2^{\circ}$  (Hudson and Thompson, 1998; Thompson and Hudson, 1999). Tropospheric column ozone at a horizontal resolution of  $5^{\circ} \times 5^{\circ}$  from 1979–1992 and 1998–2001 using the cloud-slicing method (CCD) of Ziemke et al. (2001) are compared to TTO. The ozone vertical profiles from Southern Hemisphere Additional Ozonesondes (SHADOZ) stations are also used for 1998–2000 (Thompson et al., 2003). The fire count data is estimated from the Along Tracking Scanning Radiometer (ATSR) instrument, which has a horizontal resolution of 1 km and a swath width of 512 km. Fires are identified at a fixed threshold of  $312^{\circ}$  K (Arino and Melinotte, 1995). The fire count data are averaged for the period of 1996–2000. Observations of non-gridded monthly lightning flashes from the Lightning Imaging Sensor (LIS) from daily overpasses are used in this study (Christian et al., 2003).

## 3. Results

### 3.1. Climatology of the tropical Atlantic Tropospheric Column Ozone (TCO)

Figure 1 shows the CCD 1979–1992 time-averaged seasonal TCO values over the Tropical Atlantic Ocean between  $12.5^{\circ}$  N and  $12.5^{\circ}$  S. The lowest values ( $< 34$  DU) are found during DJF and MAM and increase during the Northern Hemisphere summer and autumn seasons. The highest values ( $> 44$  DU) are found during SON over the Tropical South Atlantic Ocean in agreement with Fishman et al. (1991). Figures 2a–d show the annual cycle of 1979–1992 TCO values for the TTO and CCD datasets over the Tropical

### Space-borne observations link

G. S. Jenkins and  
J.-H. Ryu

Title Page

Abstract

Introduction

Conclusions

References

Tables

Figures

◀

▶

◀

▶

Back

Close

Full Screen / Esc

Print Version

Interactive Discussion

Atlantic Ocean (12.5° N–12.5° S, 40° W–10° E) and its various sub-regions. The annual peak in both datasets for the Tropical Atlantic Ocean occurs in September (Fig. 2a). However, there is a larger range in the annual TTO data (~17–18 DU) relative to the CCD data (8–9 DU). Furthermore the TTO values are lower than CCD values from January through May by 3–5 DU and higher than the CCD values by 3–6 DU from June through November. This pattern is also found in the sub-regions (Figs. 2b–d), except for the southern latitudinal band (12.5° S–5° S) during the June–November period when the differences between the TTO and CCD are smaller (Fig. 2b).

The TTO data suggests that some factor leads to a significant rise in TCO values beginning in June. This is also implied in the CCD dataset but the amplitude of the increase is smaller relative to TTO. A reduction in TCO values begins after the month of October. Given that the high TCO values occur over the ocean in a region of sinking motions and that there are no natural (lightning is negligible over the ocean), or anthropogenic sources located there, the ozone must be transported from remote locations.

Figures 3a, b show the TCO values in specific latitudinal zones of the Tropical Atlantic from 12.5° S to 12.5° N for the TTO and CCD ozone datasets. During the months of December through February the tropospheric column ozone values are highest between 15° S and 5° S, which is probably not due to anthropogenic sources given that biomass burning is confined to the NH. The TTO data show that ozone in the latitudes between 5° S and 5° N have the highest values from the months of April through September, while in the CCD data this latitudinal zone has the highest values from April through June. The latitudinal zone of 5° N–15° N shows a 12 DU increase in the tropospheric ozone column for TTO between May and June and the maximum values are found in July. In the CCD data the increase between May and June is less than 5 DU and the maximum value is found during July, but is approximately 6–8 DU less than the TTO value.

**Space-borne  
observations link**G. S. Jenkins and  
J.-H. Ryu

Title Page

Abstract

Introduction

Conclusions

References

Tables

Figures

◀

▶

◀

▶

Back

Close

Full Screen / Esc

Print Version

Interactive Discussion

### 3.2. Factors influencing the 1998–2001 Tropical Atlantic Tropospheric Column Ozone (TCO)

We use 1998–2001 as the period to examine Tropical Atlantic TCO values when satellite and ozonesonde data are available. Lightning, wind and fire data are used to identify sources of O<sub>3</sub> and their transport from the source regions. Figures 4 a-d show seasonal CCD TCO distribution during 1998–2001 over the Tropical Atlantic Ocean and adjacent land areas. The ozonesonde stations of Ascension Island (7.98° S, 14.42° W), Natal (5.42° S, 35.38° W) and Paramaribo (5.81° N, 55.21° W) are shown for reference. During NH winter (DJF), TCO values are higher over the Southern Tropical Atlantic Ocean and there is a relative minimum between 5–10° N, which is downstream of biomass burning in West Africa (Fig. 4a). The high TCO values in the Southern Hemisphere have been linked to lightning in Central Africa and South America (Thompson et al., 2000; Martin et al., 2002; Edwards et al., 2003).

During NH spring (MAM), TCO values are reduced over much of the SH tropics (Fig. 4b) but remain relatively high (42 DU) off the coast of Central Africa (5° S, 9° E). However, by JJA this area has expanded into the NH with the largest tropospheric column ozone values (> 42 DU) found over land areas in West Africa (7° N) and off the coast of Central Africa (7.5° S) (Fig. 4c). During SON the highest TCO values are found in the South Tropical Atlantic and extend westward over South America and eastward over Africa toward the Indian Ocean (Fig. 4d). The 1998–2001 CCD data predicts that the highest TCO values would be found at Ascension Island, followed by Natal and Paramaribo.

Figures 5a–c shows the 1998–2001 annual cycle of average ozone mixing ratios for specific layers at Ascension Island, Natal and Paramaribo based on SHADOZ ozonesonde launches. The three sites show: (a) the lowest ozone mixing are found in April or May followed by an increase during NH summer and autumn seasons. (b) The highest ozone values are found in the upper troposphere. (c) The ozone values in the lower troposphere at Paramaribo are relatively constant, while relatively large

Title Page

Abstract

Introduction

Conclusions

References

Tables

Figures

◀

▶

◀

▶

Back

Close

Full Screen / Esc

Print Version

Interactive Discussion

variations are found at Ascension Island and Natal.

The surface-150 hPa ozone mixing ratio are highest at Ascension Island followed by Natal and Paramaribo, consistent with the 1998–2001 CCD satellite estimates. The ozonesonde data also show a minimum during the month of May followed by a significant increase, which reaches its maximum value during September. There is approximately a 25–30 ppbv increase in the surface-150 hPa layer between May and September at Ascension Island. In the lower troposphere (surface-700 hPa), ozone has a minimum during April at Ascension Island and Natal and rises steeply at Ascension Island from April through July (Fig. 6b). The rise in lower tropospheric ozone is delayed slightly at Natal with the largest increase found between July and September. At Paramaribo, the ozone in the lower troposphere is highest from February through April (likely associated with biomass burning transported from Africa) and remains relatively low during the NH summer and autumn seasons.

Ozone in the middle/upper troposphere (500–150 hPa) shows a relative minimum during the month of May at each site (Fig. 6c). The ozone then increases steadily at each site reaching a maximum value in September or October. The ozone mixing ratios increase by 25–40 ppbv in the upper troposphere between May and September even at Paramaribo when biomass burning is found in the Southern Hemisphere and the values in the lower troposphere are relatively constant. The annual pattern in the upper troposphere ozonesonde data is similar to the CCD 1998–2001 TCO values when averaged over the Tropical Atlantic (12.5° S–12.5° N, 40° W–10° E) (Fig. 6d). The CCD shows a minimum in tropospheric column ozone values during May and a maximum value during September with an increase of 10 DU during this time period.

Figures 7a–d identifies fires associated with biomass burning during 1996–2000. During DJF, the fires are concentrated in the NH, reaching a minimum in MAM and then are confined to the SH during JJA. During SON, fires are found in Eastern Africa and in some parts of the Northern Hemisphere near 10° N (Fig. 7d). The pattern of fires here are consistent with the study of Duncan et al. (2003). During DJF, fires are confined primarily to West Africa, while during JJA fires are found over Africa (Central

**Space-borne  
observations link**

G. S. Jenkins and  
J.-H. Ryu

Title Page

Abstract

Introduction

Conclusions

References

Tables

Figures

◀

▶

◀

▶

Back

Close

Full Screen / Esc

Print Version

Interactive Discussion

---

**Space-borne  
observations link**

G. S. Jenkins and  
J.-H. Ryu

---

Title Page

Abstract

Introduction

Conclusions

References

Tables

Figures

◀

▶

◀

▶

Back

Close

Full Screen / Esc

Print Version

Interactive Discussion

© EGU 2003

and Eastern) and South America (Brazil). However, during JJA the fires are not located near the Equator or Northern Hemisphere Tropics where TCO values are increasing (Fig. 4). This is especially true near the coast of West Africa where high TCO values are found during JJA. Biomass burning from Central Africa is a likely candidate for the increase in lower tropospheric ozone mixing ratios that are found at Ascension Island from JJA through SON (Fig. 6b). Biomass burning in Central Africa that is transported by easterly winds is also likely the cause for increasing the lower troposphere ozone mixing ratios in Natal from June through September (Kirchhoff et al., 1996).

During SON, fires are confined primarily to eastern parts of Africa and South America (Brazil) (Fig. 7d). Consequently, any significant contributions of biomass burning from these regions to the SON Tropical Atlantic Ozone Maximum must require long-range transport (> 1000 km). Another source of ozone, especially in the middle/upper troposphere is lightning via NO<sub>x</sub> production shown in the following reactions:

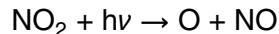
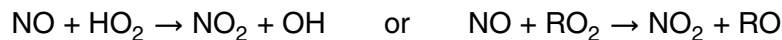


Figure 8a shows that the total number of flashes for land areas (South America and Africa) in latitudes between 15° S–15° N and longitudes 80° W–30° E for the period of 1998–2001 as detected from LIS overpasses. The smallest and largest numbers of flashes occur during DJF and SON, respectively. Figure 8b shows that during DJF the majority of lightning flashes are from the latitudinal zones of 15° S–5° S and 5° S–5° N. During MAM there is a poleward shift in lightning flashes with majority occurring in the zones of 5° S–5° N and 5° S–15° N. During JJA, the period when TOC values begin to increase substantially, the largest numbers of flashes are found in the latitude band of 5° N–15° N. During SON, when TOC values are highest over the Tropical Atlantic Ocean a large number of flashes are found at all three latitude zones. Over the annual cycle, the latitudes of 15° S–5° S produce the largest number of flashes from October

**Space-borne  
observations link**G. S. Jenkins and  
J.-H. Ryu

Title Page

Abstract

Introduction

Conclusions

References

Tables

Figures

◀

▶

◀

▶

Back

Close

Full Screen / Esc

Print Version

Interactive Discussion

© EGU 2003

through January (NH autumn/winter) (Fig. 8c). The latitude band of 5° S–5° S produces the largest number of flashes from February through April (NH winter/spring) and the latitude band of 5° N–15° N produces the largest number of flashes from May through September (NH late spring/summer/early autumn). This time period overlaps with the significant increase in TOC values from the TOMS satellite measurements.

During DJF, MAM and JJA the majority (> 60%) of lightning flashes are associated with the African continent (Fig. 9a). During SON the distribution of lightning flashes between Africa and South America is nearly equal. Figures 9b–d show the number of lightning flashes in the three latitude zones for the continents of Africa and South America during 1998–2001. In the most southern latitudes (15° S–5° S), there are more flashes in South America in three of the four seasons with the exception of MAM. The opposite pattern is found in the other two latitude zones (5° S–5° N and 5° N–15° N) where lightning in Africa is dominant throughout the year when compared to South America (Figs. 9c, d). These results are consistent with lightning distribution by the Optical Transient Detector (OTD) (Christian et al 2003). They show that the highest flash densities are found in Central Africa followed by regions in South America. The number of lightning flashes is lower by a factor of 4–5 during MAM relative to SON for South America in the latitude zones of 15° S–5° S (Fig. 9b). This implies that there is either less convective activity or that convective intensity is reduced during MAM relative to SON in South America. It is also possible that aerosols from biomass burning during SON can alter the microphysical properties (possibly serving as ice nuclei) of deep convection leading to more lightning.

Figures 10–13 show the DJF, MAM, JJA and SON middle/upper tropospheric zonal winds and streamlines at 500, 400, 300, 200 hPa during 1998–2001. The ozonesonde stations of Ascension Island, Natal, and Paramaribo are shown for reference. Easterly winds are persistent over the Tropical Atlantic at 500, 400 hPa during all seasons with a migration toward the Northern Hemisphere from DJF through JJA (Figs. 10–13a, b). This wind pattern would be conducive to the westward transport of NO<sub>x</sub> and O<sub>3</sub> associated with lightning from Central Africa (15° S–5° N) during DJF, MAM and SON and from

---

**Space-borne  
observations link**G. S. Jenkins and  
J.-H. Ryu

---

[Title Page](#)[Abstract](#)[Introduction](#)[Conclusions](#)[References](#)[Tables](#)[Figures](#)[◀](#)[▶](#)[◀](#)[▶](#)[Back](#)[Close](#)[Full Screen / Esc](#)[Print Version](#)[Interactive Discussion](#)

© EGU 2003

West Africa (5° N–15° N) during JJA. At lower pressure levels (300, 200 hPa), westerly winds become more important during DJF, MAM and SON making South America a potential source of ozone enrichment via lightning in the upper troposphere (Figs. 10–13c, d).

5 During DJF, the ozonesonde stations are under the influence of 200° hPa westerly winds, which originate over South America and have been linked to elevated tropical Atlantic ozone via lightning (Edwards et al., 2003). A similar wind pattern also exists during MAM at 200 hPa when lightning in South America is less frequent and could help to explain why upper troposphere ozone mixing ratios are significantly reduced at  
10 the three ozonesonde stations during this period (Fig. 5). Moreover, it would explain why TCO values in the western Atlantic near South America are significantly reduced between DJF and MAM (Figs. 4a, b). During SON the ozonesonde stations are under the influence of westerly winds from South America when lightning is the most frequent and should contribute to elevated ozone mixing ratios in the upper troposphere.

15 During JJA, however, easterly flow is dominant in the upper troposphere and is associated with the 200 hPa Tropical Easterly Jet (TEJ), which crosses much of Africa from India (Fig. 12d). Consequently, O<sub>3</sub> and NO<sub>x</sub> enrichment over the Tropical Atlantic and at the ozonesonde stations is likely associated with lightning activity over West Africa.

#### 4. Summary and discussion

20 In this paper we have examined the annual evolution of tropospheric ozone over the Tropical Atlantic in connection to biomass burning, lightning and large-scale transport with an emphasis on 1998–2001. Our findings show:

- The highest TCO values are found in the hemisphere opposite of biomass burning during DJF and JJA (Tropical Ozone Paradox). During DJF, biomass burning is concentrated in the Northern Hemisphere (West Africa), but elevated ozone levels  
25 over the South Tropical Atlantic are due to lightning (NO<sub>x</sub> production) in South

---

**Space-borne  
observations link**G. S. Jenkins and  
J.-H. Ryu

---

[Title Page](#)[Abstract](#)[Introduction](#)[Conclusions](#)[References](#)[Tables](#)[Figures](#)[◀](#)[▶](#)[◀](#)[▶](#)[Back](#)[Close](#)[Full Screen / Esc](#)[Print Version](#)[Interactive Discussion](#)

© EGU 2003

America and Central Africa. During JJA, biomass burning is concentrated in the Southern Hemisphere (southern sector of Central Africa, South America), but elevated ozone levels over the Equatorial Atlantic ( $5^{\circ}$  S– $10^{\circ}$  N) are probably due to lightning ( $\text{NO}_x$  production) in West Africa and Central Africa to a lesser extent.

- 5 – During MAM, the highest tropospheric column ozone values are found off the western coast of Central Africa and are caused by lightning and the production of  $\text{NO}_x$  over Central Africa. Biomass burning is at a minimum in Africa and South America during MAM.
- 10 – In the latitude zone of  $15^{\circ}$  S– $15^{\circ}$  N, the majority of lightning flashes are from Africa except during SON. During SON, the majority of lightning flashes occurring in the latitudinal zone of  $15^{\circ}$  S– $5^{\circ}$  S are from South America.
- 15 – During SON, lightning from South America, West and Central Africa combine to produce the Tropical Atlantic Ozone Maximum. However, the conditions leading up to the SON Tropical Atlantic Ozone Maximum develop during JJA. Biomass burning in South America and Eastern Africa and its subsequent transport to the Tropical Atlantic Ocean is also an important factor (Jenkins et al., 1997).

A number of observational studies have suggested that the high ozone in the troposphere primarily during Northern Hemisphere Autumn (SON) is associated with biomass burning in Africa and South America. This may be true in the lower troposphere but does not necessarily explain the high ozone mixing ratios that are typically found in the upper troposphere (Weller et al., 1996). One can explain these high values through biomass burning if there is deep convection, which can vent pollutants from the Planetary Boundary Layer into the upper troposphere. This may be the case for South America and Southeastern Africa where low level winds in South America and Central Africa can transport pollutants westward into regions of deep convection (Kirchhoff et al., 1996; Jenkins et al., 1997; Jenkins, 2000). Weller et al. (1996) suggests that stratospheric intrusions of air could also explain high values in the upper troposphere. Such

intrusions could take place through the entrainment of stratospheric air associated with deep convection.

Our analysis presents a slightly different version of the Tropical Atlantic Ozone Maximum during SON. We suggest that lightning, based on LIS observations, is to a first order approximation responsible for the tropospheric ozone maximum with long-range transport of pollutants and stratospheric intrusions being secondary. Even if these other processes are important to enriching tropospheric ozone they are associated with deep convective processes, which includes lightning. Observations of  $\text{NO}_x$  and  $\text{O}_3$  production associated with deep convection are limited but show that the vertical transport of ozone/ozone precursors, stratospheric intrusions,  $\text{NO}_x$  and  $\text{O}_3$  production via lightning do occur (Poulida et al., 1996; Pickering et al., 1996; Stith et al., 1999; Dye et al., 1999). The study of DeCaria et al. (2000) found an ozone production of  $7 \text{ ppbv d}^{-1}$  from a simulated thunderstorm in the United States where elevated  $\text{NO}_x$  was observed. Thompson et al. (2000) suggests an ozone production of  $4\text{--}8 \text{ ppbv d}^{-1}$  during the Aerosols99 campaign originating from lightning in Central Africa. Ozone production during SON adjacent to the Tropical Atlantic may be considerably higher given three regional sources (South America, Central Africa, West Africa) for lightning. The modeling study of Moxin and Levy (2000), suggests that lightning is responsible for the Tropical South Atlantic tropospheric ozone maximum during SON. The modeling study of Martin et al. (2002) suggests a  $10\text{--}14 \text{ DU}$  enhancement of ozone from lightning.

Some challenges to the modeling community are simulating deep convective processes and lightning events. In order to examine deep convective processes associated with vertical transports of ozone/ozone precursors, global climate models or mesoscale models with fine horizontal resolutions ( $10\text{--}20 \text{ km}$  for non-hydrostatic conditions) will be necessary. In Jenkins et al. (1997), deep convective processes were examined at 99, 33 and 11 km grid spacing. The most vigorous convection with vertical velocities greater than  $10 \text{ m/s}$  was found using the 11 km grid. Strong updrafts are also a requirement for diagnostic or prognostic modeling of lightning. The sim-

**Space-borne  
observations link**

G. S. Jenkins and  
J.-H. Ryu

Title Page

Abstract

Introduction

Conclusions

References

Tables

Figures

◀

▶

◀

▶

Back

Close

Full Screen / Esc

Print Version

Interactive Discussion

---

**Space-borne  
observations link**G. S. Jenkins and  
J.-H. Ryu

---

[Title Page](#)[Abstract](#)[Introduction](#)[Conclusions](#)[References](#)[Tables](#)[Figures](#)[◀](#)[▶](#)[◀](#)[▶](#)[Back](#)[Close](#)[Full Screen / Esc](#)[Print Version](#)[Interactive Discussion](#)

© EGU 2003

ulation of mixed phased precipitation, however, is also a significant requirement for lightning production. Very fine GCM simulations are unlikely in the near future and mesoscale/cloud resolving models will only give a limited view of modeled deep convection and lightning. Mixed phase physics, however, can be incorporated into GCMs, which will provide some diagnostic or prognostic measures of lightning processes although the vertical velocities will tend to be underestimated.

Martin et al. (2002) suggests that satellite derived tropospheric column ozone values are significantly overestimates when compared with MOSAIC data during JJA. However, the ozonesonde data shows a pattern that is consistent with the satellite measurement with a significant rise in ozone values after the month of May. The rise in ozone mixing ratios is most pronounced in the middle/upper troposphere making lightning a likely cause. Drummond et al. (1988) also found enhanced upper troposphere  $\text{NO}_x$  values, indirectly supporting the satellite TOC estimates, during the month of June over the Tropical Atlantic Ocean and suggested that lightning processes over continents may have been responsible. During JJA, we have found that lightning over West Africa is likely a significant contributor to  $\text{NO}_x$  and the subsequent production of  $\text{O}_3$ . Recent studies (Mohr and Zipser, 1996; Nesbitt et al., 2000; Toracinta and Zipser, 2001; Sealy et al., 2003) using the data from the polar orbiting satellites and the TRMM satellite (Kummerow et al., 1998) have examined precipitation and lightning properties, using the Optical Transient Detector (OTD) and (LIS) data, in the tropics and West Africa. Nesbitt et al. (2000), show that lightning is typically associated with precipitation features that contain a significant ice content. Mesoscale convective systems (MCSs), which include squall line, mesoscale convective complexes and non-squall tropical clusters, have low polarization temperatures because of their high ice content in Africa. Moreover, MCSs were identified with the largest number of lightning flashes in Africa and South America (Nesbitt et al., 2000).

Sealy et al. (2003) have found that the region closest to the Sahara desert – the Sahel ( $10\text{--}18^\circ\text{N}$ ), produced the highest number of flashes relative to the wetter Guinea region ( $5\text{--}10^\circ\text{N}$ ) during May–September 1998–2000. A higher frequency of lightning

**Space-borne  
observations link**G. S. Jenkins and  
J.-H. Ryu

Title Page

Abstract

Introduction

Conclusions

References

Tables

Figures

◀

▶

◀

▶

Back

Close

Full Screen / Esc

Print Version

Interactive Discussion

© EGU 2003

flashes in the Sahel occurred at night, which is consistent with studies of MCSs showing a distinct diurnal pattern, with the largest mean radius occurring between 18:00 and 22:00 LST (Mathon and Laurent, 2000). Consequently, nighttime lightning may lead to an accumulation of  $\text{NO}_2$ ,  $\text{NO}_3$  and  $\text{NO}_2\text{O}_5$  until sunrise of the next day thereby serving as a source of ozone in the absence of deep convection. Moreover, there may be a direct link between lightning, ice content and aerosols. In the case of West Africa, the aerosols come from Saharan dust and would serve as ice nuclei in updrafts of developing convective cells. Strong vertical motions, ice particles, graupel and super-cooled water would be associated with the high flash rates found in the Sahel, thereby enriching upper troposphere  $\text{NO}_x$  and ozone mixing ratios. Demott et al. (2003) have found high concentrations of ice nuclei in Saharan dust and show that the ice nuclei concentrations exceeded the typical values by a factor of 20 to 100.

The results presented in this paper imply that increases in TOC values during JJA as implied by satellite estimates are real and caused by lightning. There is an opportunity to determine the cause for the discrepancies between satellite estimated TOCs and the MOSAIC data during the Northern Hemisphere summer season. The proposed African Monsoon Multidisciplinary Experiment (AMMA) in West Africa, which has a summer special observing period (<http://medias.obs-mip.fr/amma>) during JJA of 2006, could help to resolve this issue. This can be achieved through the launch of ozonesondes, ship and aircraft measurements of  $\text{O}_3$  and  $\text{NO}_x$  and concurrent satellite measurements.

*Acknowledgements.* This research was supported through NSF Grant ATM-0105206 and NASA Grant NAG5-7443. Lightning data provided by the NASA Lightning Imaging Sensor (LIS) science team and the LIS data center located at the Global Hydrology and Climate Center (GHCC), Huntsville, Alabama, USA.

**References**

Arino, O. and Melinotte, J.-M.: The Fire Atlas, Earth Observation Quarterly, 50, 1995.

---

**Space-borne  
observations link**G. S. Jenkins and  
J.-H. Ryu

---

[Title Page](#)[Abstract](#)[Introduction](#)[Conclusions](#)[References](#)[Tables](#)[Figures](#)[◀](#)[▶](#)[◀](#)[▶](#)[Back](#)[Close](#)[Full Screen / Esc](#)[Print Version](#)[Interactive Discussion](#)

© EGU 2003

Christian, H. J., Blakeslee, R. J., Boccippio, D. J. et al.: Global frequency and distribution of lightning as observed from space by the Optical Transient Detector, *J. Geophys. Res.*, 108, doi:10.1029/2002JD002347, 2003.

DeCaria, A. J., Pickering, K. E., Stenchikov, G. L., Scala, J. R., Stith, J. L., Dye, J. E., Ridley, B. A., and Laroche, P.: A cloud-scale model study of lightning-generated  $\text{NO}_x$  in an individual thunderstorm during STERAO-A, *J. Geophys. Res.*, 105, 11 601–11 616, 2000.

Demott, P. J., Sassen, K., Peollot, M. R. et al.: African dust aerosols as atmospheric ice nuclei, *GRL*, 30, doi:10.1029/2003/GL017410, 2003.

Drummond, J. W., Ehhalt, D. H., and Volz, A.: Measurements of Nitric Oxide between 0–12 km altitude and 67° N to 60° S latitude obtained during STRATOZ III, *J. Geophys. Res.*, 93, 15 831–15 849, 1988.

Duncan, B. N., Martin, R. V., Staudt, A. C., Yevich, R., and Logan, J. A.: Interannual and seasonal variability of biomass burning emissions constrained by satellite observations, *J. Geophys. Res.*, 108, doi:10.1029/2002JD002378, 2003.

Dye, J. E., Ridley, B. A., Skamarock, W. et al.: An Overview of the STERAO-Deep Convection Experiment with Results for the 10 July Storm, *J. Geophys. Res.*, 105, 10 023–10 045, 1999.

Edwards D. P., Lamarque, J.-F., Attie, J.-L. et al.: Tropospheric Ozone over the Tropical Atlantic: A satellite perspective, *J. Geophys. Res.*, 108, doi:10.1029/2002JD002927, 2003.

Fishman, J., Fakhruzzaman, K., Cros, B., and Nganga, D.: Identification of Widespread Pollution in the Southern Hemisphere Deduced from Satellite Analyses, *Science*, 252, 1693–1693, 1991.

Fishman, J., Hoell Jr., J. M., Bendura, R. D., McNeal, R. J., and Kirchhoff, V. W. J. H.: NASA GTE TRACE A Experiment (September–October 1992): Overview, *J. Geophys. Res.*, 101, 23 865–23 879, 1996.

Hudson, R. D. and Thompson, A. M.: Tropical tropospheric ozone from total mapping spectrometer by a modified-residual method, *J. Geophys. Res.*, 103, 22 129–22 145, 1998.

Jacob D. A., Heikes, B. G., Fan, S.-M. et al.: Origin of ozone and  $\text{NO}_x$  in the tropical troposphere: A photochemical analysis of aircraft observations over the South Atlantic basin, *J. Geophys. Res.*, 101, 24 069–24 082, 1996.

Jenkins, G. S., Mohr, K., Morris, V. R., and Arino, O.: The Role of Convective Processes over the Zaire and Congo Basins to the Southern Hemisphere Ozone Maximum, *J. Geophys. Res.*, 102, 18 963–18 980, 1997.

Jenkins, G. S.: TRMM satellite estimates of convective processes in Central Africa during

---

**Space-borne  
observations link**

---

G. S. Jenkins and  
J.-H. Ryu

---

[Title Page](#)[Abstract](#)[Introduction](#)[Conclusions](#)[References](#)[Tables](#)[Figures](#)[◀](#)[▶](#)[◀](#)[▶](#)[Back](#)[Close](#)[Full Screen / Esc](#)[Print Version](#)[Interactive Discussion](#)

© EGU 2003

- September, October, November 1998: implications for elevated Atlantic tropospheric ozone, *GRL*, 27, 1711–1714, 2000.
- Kalnay, E. M., Kanamitsu, M., Kistler, R. et al.: The NCEP/NCAR 40-Year Reanalysis Project, *Bulletin of the American Meteorological Society*, 77, 3, 437–472, 1996.
- 5 Kim, J. H., Newchurch, M. J., and Han, K.: Distribution of Tropical Ozone Determined by the Scale-Angle Method Applied to TOMS Measurements, *JAS*, 58, 2699–2708, 2001.
- Kirchhoff, V. W. J. H, Alves, J. R., Da Silva, F. R., and Fishman, J: Observations of ozone concentrations in the Brazilian cerrado during the TRACE A field expedition, *J. Geophys. Res.*, 101, 24 029–24 042, 1996.
- 10 Kummerow, C., Barnes, W., Kozu, T., Shiue, J., and Simpson, J.: The Tropical Rainfall Measuring Mission (TRMM) sensor package, *J. Atmos. Oceanic Technol.*, 15, 809–817, 1998.
- Martin, R. V., Jacob, D. J., Logan, J. A. et al.: Interpretation of TOMS observations of tropical tropospheric ozone with a global model and in situ observations, *J. Geophys. Res.*, 107, DOI:10.1029/2001JD001480, 2002.
- 15 Mathon, V. and Laurent, H.: Life cycle of Sahelian mesoscale convective cloud systems, *Q. J. R. Meteorol. Soc.*, 127, 377–406, 2001.
- Mohr, K. I. and Zipser, E. J.: Defining mesoscale convective systems by the 85-GHz ice scattering signatures, *BAMS*, 77, 1179–1188, 1996.
- Moxim, W. J. and Levy II, H.: A model analysis of the tropical South Atlantic Ocean tropospheric ozone maximum: The interaction of transport and chemistry, *J. Geophys. Res.*, 105, 17 393–17 415, 2000.
- 20 Nesbitt, S. W., Zipser, E. J., and Cecil, D. J.: A census of precipitation features in the tropics using TRMM: Radar, ice scattering and lightning observations. *J. Clim*, 13, 4087–4106, 2000.
- Pickering, K. E., Thompson, A. M., Wang, Y. et al.: Convective transport of biomass burning emissions over Brazil during TRACE-A, *J. Geophys. Res.*, 101, 23 993–24 012, 1996.
- 25 Poulida, O., Dickerson, R. R., and Heymsfield, A.: Stratosphere-troposphere exchange in a mid-latitude mesoscale convective complex, 1, *Observations*, *J. Geophys. Res.*, 101, 6823–6836, 1996.
- Rosenfeld, D.: TRMM observed direct evidence of Smoke from Forest Fire Inhibiting Rainfall, *GRL*, 26, 3105–3108, 1999.
- 30 Sealy A., Jenkins, G. S., and Walford, S. C.: Seasonal/regional comparisons of rain rates and rain characteristics in West Africa using TRMM observations, *J. Geophys. Res.*, 108, DOI 10.1029/2002JD002667, 2003.

---

**Space-borne  
observations link**G. S. Jenkins and  
J.-H. Ryu

---

[Title Page](#)[Abstract](#)[Introduction](#)[Conclusions](#)[References](#)[Tables](#)[Figures](#)[◀](#)[▶](#)[◀](#)[▶](#)[Back](#)[Close](#)[Full Screen / Esc](#)[Print Version](#)[Interactive Discussion](#)

© EGU 2003

Stith, J., Dye, J. E., Ridley, B. et al.: NO signatures from lightning flashes, *J. Geophys. Res.*, 104, 16 081–16 089, 1999.

Thompson, A. M., Pickering, K. E., McNamara, D. P. et al.: Where did tropospheric ozone over southern Africa and the tropical Atlantic come from in October 1992? Insights from TOMS, GTE TRACE A and SAFARI 1992, *J. Geophys. Res.*, 101, 24 251–24 278, 1996.

Thompson, A. M. and Hudson R. D.: Tropical tropospheric ozone (TTO) Maps from Nimbus 7 and Earth-Probe TOMS by the modified-residual method: Evaluation with sondes, ENSO signals and trends from Atlantic regional time series, *J. Geophys. Res.*, 104, 26 961–26 975, 1999.

Thompson, A. M., Doddridge, B. G., Witte, J. C. et al.: A Tropical Atlantic Paradox: Shipboard and Satellite Views of a Tropospheric Ozone Maximum and Wave-one in January–February 1999, *GRL*, 27, 3317–3320, 2000.

Thompson, A. M., Witte, J. C., McPeters, R. D. et al.: Southern Hemisphere Additional Ozonesondes (SHADOZ) 1998–2000 tropical ozone climatology. 1. Comparison with Total Ozone Mapping Spectrometer (TOMS) and ground-based measurements, *J. Geophys. Res.*, 108, doi:10.1029/2001JD000967, 2003.

Toracinta, E. R. and Zipser, E. J.: Lightning and SSM/I ice-scattering mesoscale convective systems in the global tropics, *J. Appl. Met.*, 40, 983–1002, 2001.

Weller, R., Lilischkis, R., Schrems, O., Neuber, R., and Wessel, S.: Vertical ozone distribution in the marine atmosphere over the central Atlantic Ocean (56° S–50° N), *J. Geophys. Res.*, 101, 1387–1399, 1996.

CCD Tropospheric Ozone 1979-1992 (DU)

Space-borne observations link

G. S. Jenkins and  
J.-H. Ryu

Title Page

Abstract

Introduction

Conclusions

References

Tables

Figures

◀

▶

◀

▶

Back

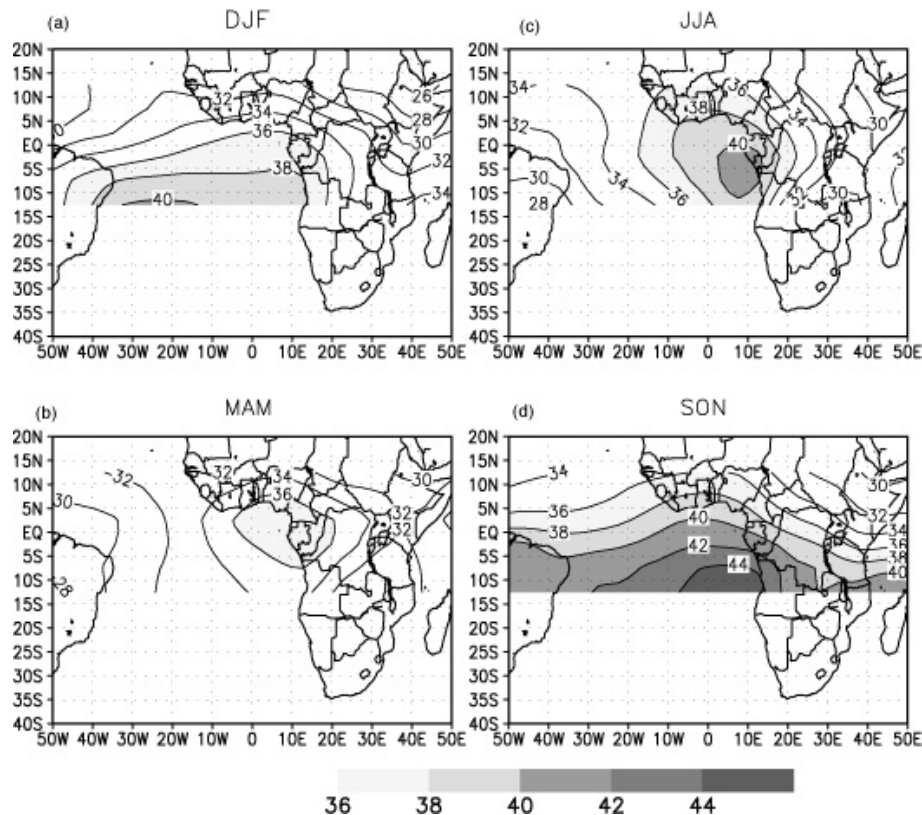
Close

Full Screen / Esc

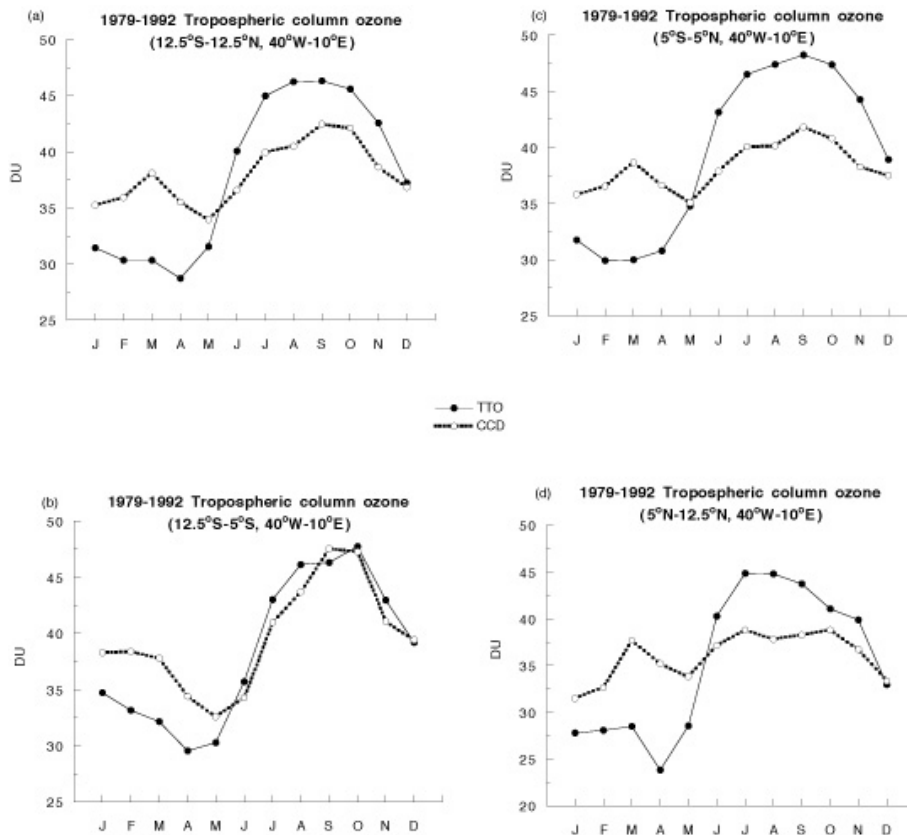
Print Version

Interactive Discussion

© EGU 2003



**Fig. 1.** Climatological (1979–1992) CCD Tropospheric Column Ozone values **(a)** DJF, **(b)** MAM, **(c)** JJA, **(d)** DJF. Units are Dobsons.



**Fig. 2.** The annual cycle of the tropospheric column ozone (1979–1992) for TTO and CCD averaged over (a) 12.5°S–12.5°N, 40°W–10°E, (b) 12.5°S–5°S, 40°W–10°E, (c) 5°S–5°N, 40°W–10°E, (d) 5°N–12.5°N, 40°W–10°E. Units are Dobsons.

[Print Version](#)[Interactive Discussion](#)

© EGU 2003

Space-borne observations link

G. S. Jenkins and J.-H. Ryu

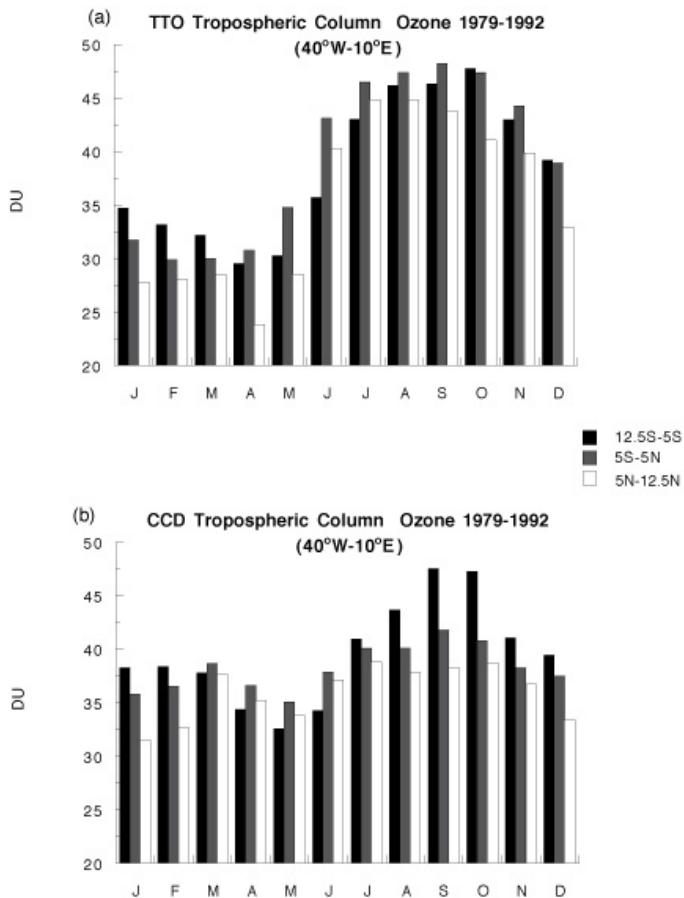


Fig. 3. The annual cycle of the tropospheric column ozone (1979–1992) by latitude zones for (a) TTO and (b) CCD. Units are Dobsons.

Title Page

Abstract Introduction

Conclusions References

Tables Figures

⏪ ⏩

◀ ▶

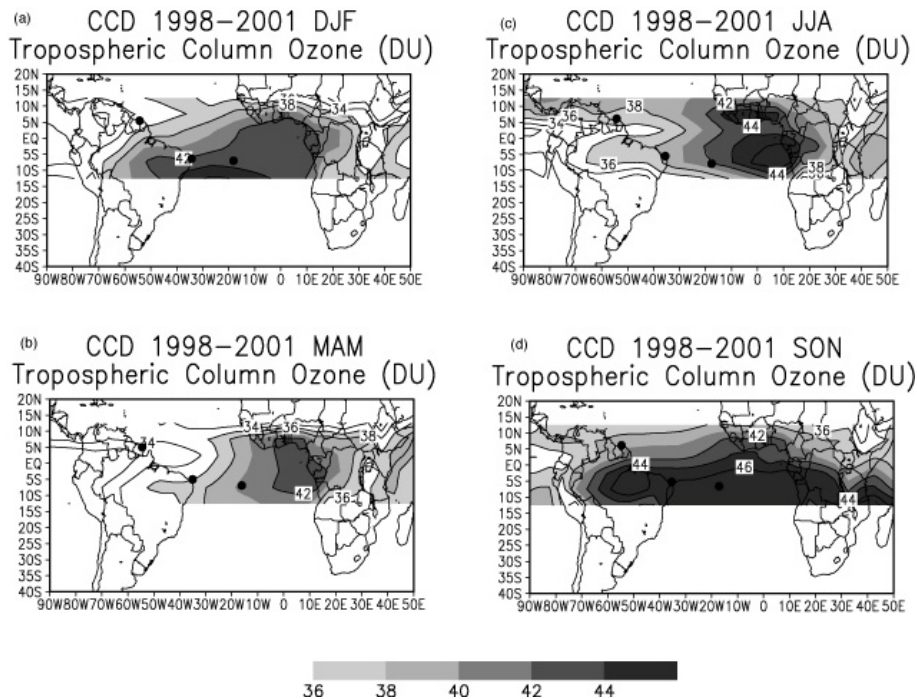
Back Close

Full Screen / Esc

Print Version

Interactive Discussion

**Space-borne  
observations link**

 G. S. Jenkins and  
J.-H. Ryu


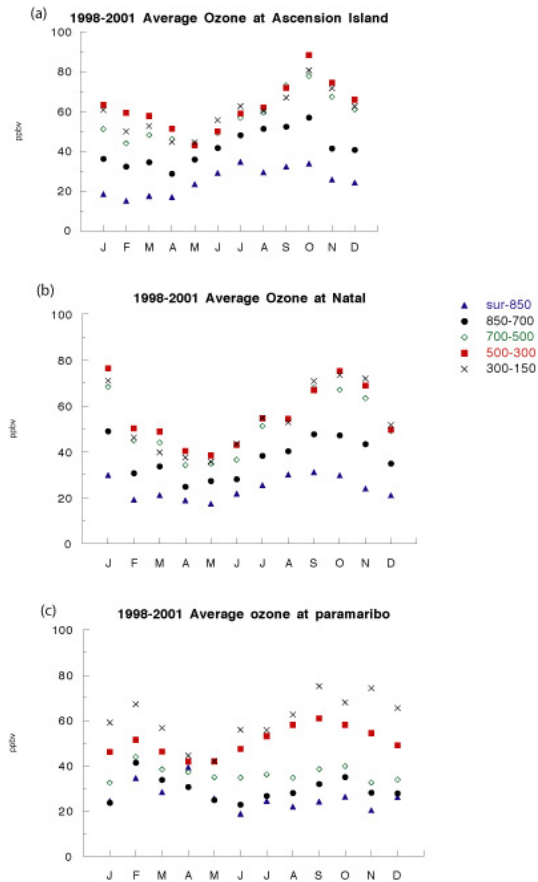
**Fig. 4.** 1998–2001 CCD Tropospheric Column Ozone values (a) DJF, (b) MAM, (c) JJA, (d) DJF. Units are Dobsons.

[Title Page](#)
[Abstract](#)
[Introduction](#)
[Conclusions](#)
[References](#)
[Tables](#)
[Figures](#)
[◀](#)
[▶](#)
[◀](#)
[▶](#)
[Back](#)
[Close](#)
[Full Screen / Esc](#)
[Print Version](#)
[Interactive Discussion](#)

© EGU 2003

Space-borne observations link

G. S. Jenkins and J.-H. Ryu



**Fig. 5.** 1998–2001 average ozone mixing ratios in various tropospheric layers. **(a)** Ascension Island, **(b)** Natal, **(c)** Paramaribo. Units are ppbv.

Title Page

Abstract

Introduction

Conclusions

References

Tables

Figures

◀

▶

◀

▶

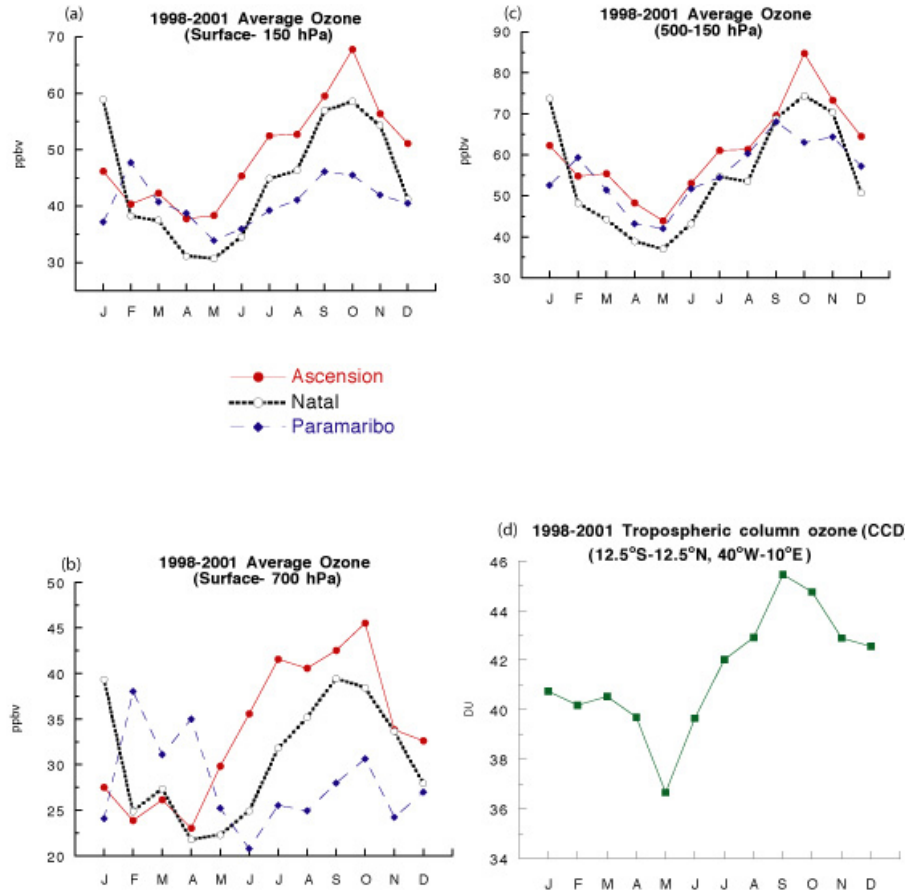
Back

Close

Full Screen / Esc

Print Version

Interactive Discussion

Space-borne  
observations linkG. S. Jenkins and  
J.-H. Ryu

**Fig. 6.** 1998–2001 average ozone mixing ratios (ppbv) at Ascension Island, Natal and Paramaribo from **(a)** surface to 150 hPa, **(b)** Surface to 700 hPa, **(c)** 500 to 150 hPa. **(d)** 1998–2001 CCD tropospheric column ozone for 12.5° S–12.5° N, 40° W–10° E.

Title Page

Abstract

Introduction

Conclusions

References

Tables

Figures

◀

▶

◀

▶

Back

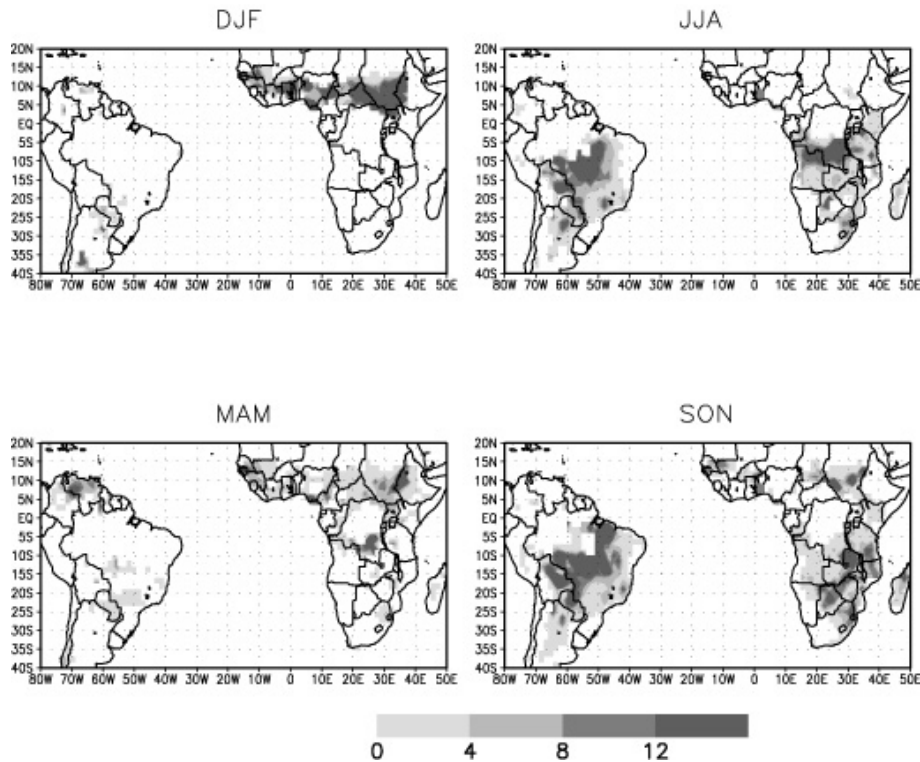
Close

Full Screen / Esc

Print Version

Interactive Discussion

## Month composite of ATSR fire counts: 1996–2000



**Fig. 7.** ATSR fire count during 1996–2000 for: (a) DJF, (b) MAM, (c) JJA, (d) DJF. Number of fires per pixel.

**Space-borne  
observations link**

G. S. Jenkins and  
J.-H. Ryu

Title Page

Abstract

Introduction

Conclusions

References

Tables

Figures

◀

▶

◀

▶

Back

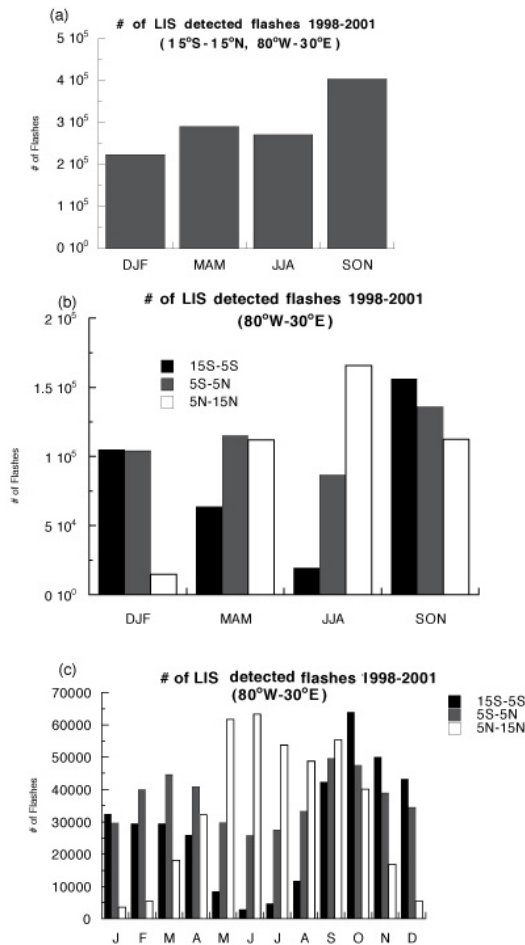
Close

Full Screen / Esc

Print Version

Interactive Discussion

© EGU 2003



**Fig. 8.** 1998–2001 LIS seasonal lightning statistics: **(a)** total number of seasonal flashes **(b)** distribution of seasonal flashes for latitude zones of 15° S–5° S, 5° S–5° N, 5° N–15° N, **(c)** distribution of monthly flashes for latitude zones of 15° S–5° S, 5° S–5° N, 5° N–15° N.

Title Page

Abstract

Introduction

Conclusions

References

Tables

Figures

⏪

⏩

◀

▶

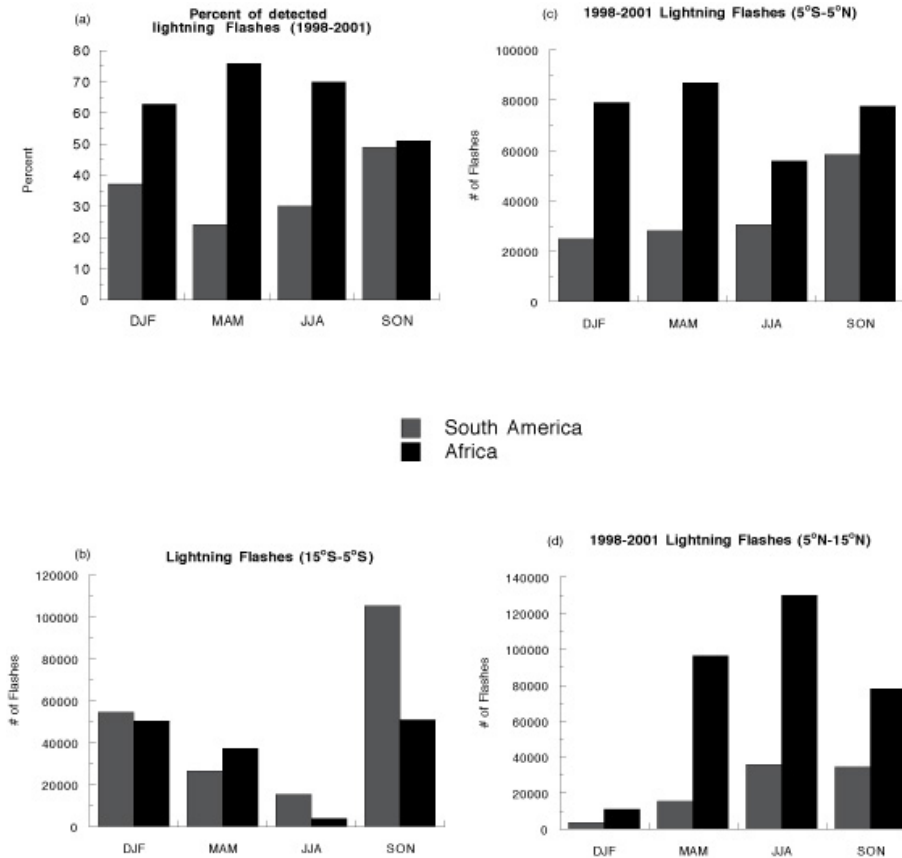
Back

Close

Full Screen / Esc

Print Version

Interactive Discussion



**Fig. 9.** (a) Percentage of seasonal flashes in South America and Africa, (b) number of detected lightning flashes in 15° S–5° S for Africa and South America, (c) number of detected lightning flashes in 5° S–5° N for Africa and South America, (d) number of detected lightning flashes in 5° N–15° N for Africa and South America.

Title Page

Abstract

Introduction

Conclusions

References

Tables

Figures

◀

▶

◀

▶

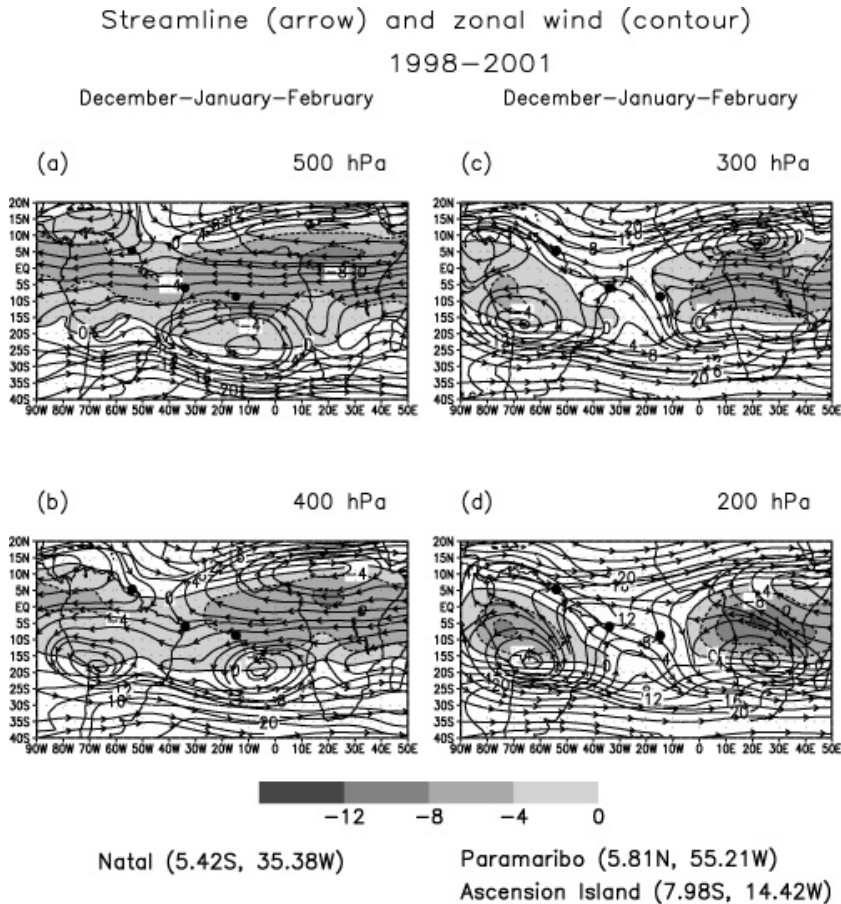
Back

Close

Full Screen / Esc

Print Version

Interactive Discussion



### Space-borne observations link

G. S. Jenkins and  
J.-H. Ryu

Title Page

Abstract

Introduction

Conclusions

References

Tables

Figures

◀

▶

◀

▶

Back

Close

Full Screen / Esc

Print Version

Interactive Discussion

© EGU 2003

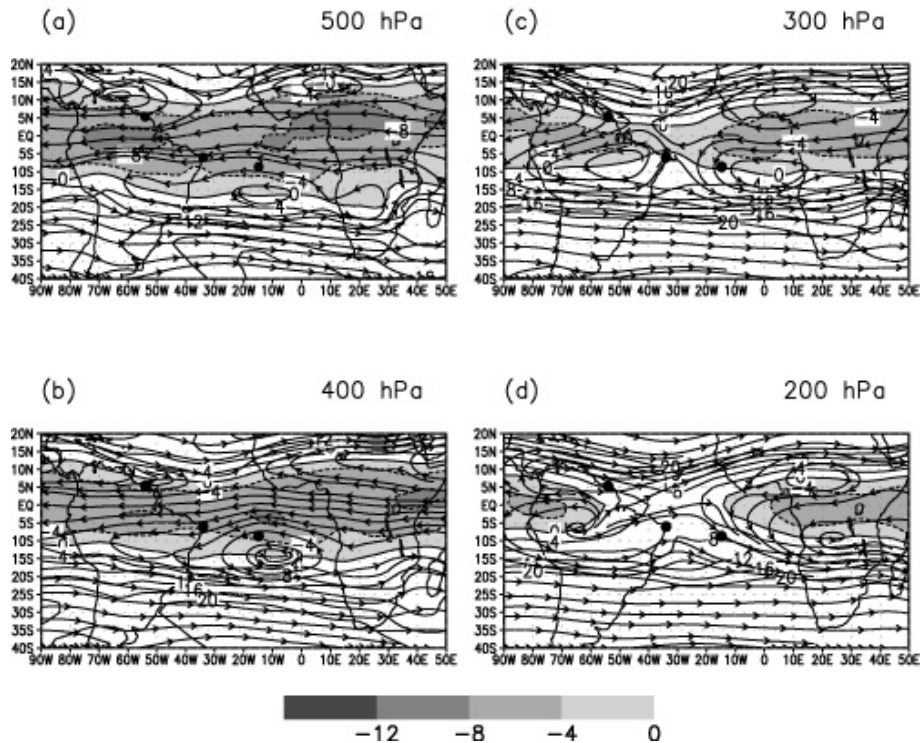
**Fig. 10.** 1998–2001 DJF middle/upper troposphere zonal winds and streamlines for (a) 500 hPa, (b) 400 hPa, (c) 300 hPa, (d) 200 hPa. Shaded regions are easterly winds. Units are  $\text{m}\cdot\text{s}^{-1}$ .

## Streamline (arrow) and zonal wind (contour)

1998–2001

March–April–May

March–April–May



**Fig. 11.** 1998–2001 MAM middle/upper troposphere zonal winds and streamlines for (a) 500 hPa, (b) 400 hPa, (c) 300 hPa, (d) 200 hPa. Shaded regions are easterly winds. Units are  $\text{m}\cdot\text{s}^{-1}$ .

### Space-borne observations link

G. S. Jenkins and  
J.-H. Ryu

[Title Page](#)
[Abstract](#)
[Introduction](#)
[Conclusions](#)
[References](#)
[Tables](#)
[Figures](#)
[◀](#)
[▶](#)
[◀](#)
[▶](#)
[Back](#)
[Close](#)
[Full Screen / Esc](#)
[Print Version](#)
[Interactive Discussion](#)

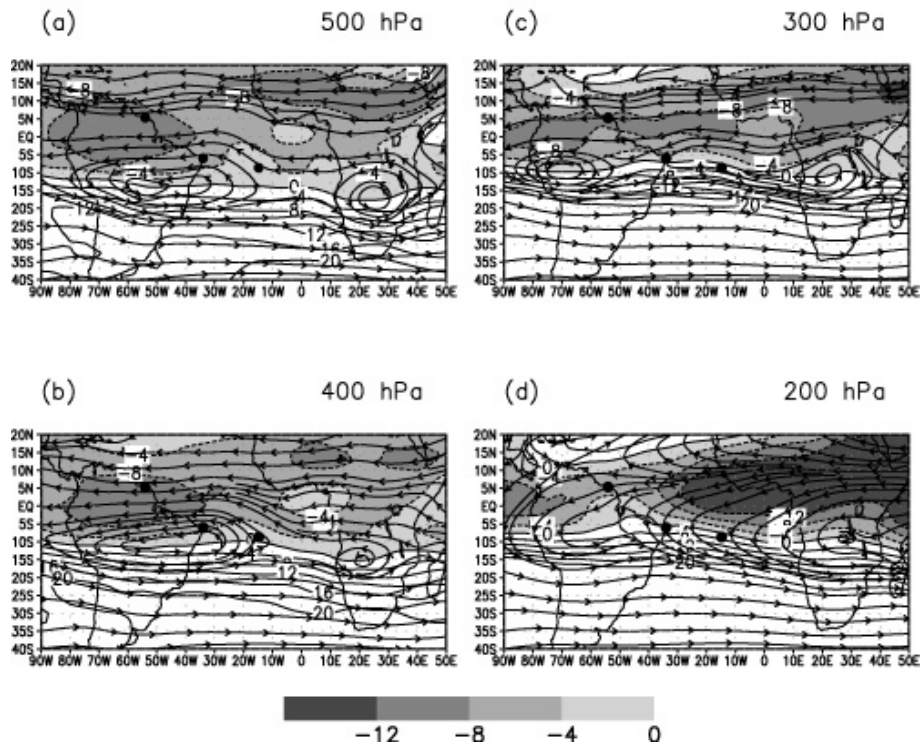
© EGU 2003

# Streamline (arrow) and zonal wind (contour)

1998–2001

June–July–August

June–July–August



**Fig. 12.** 1998–2001 JJA middle/upper troposphere zonal winds and streamlines for **(a)** 500 hPa, **(b)** 400 hPa, **(c)** 300 hPa, **(d)** 200 hPa. Shaded regions are easterly winds. Units are  $\text{m}\cdot\text{s}^{-1}$ .

ACPD

3, 5725–5754, 2003

Space-borne  
observations link

G. S. Jenkins and  
J.-H. Ryu

Title Page

Abstract

Introduction

Conclusions

References

Tables

Figures

◀

▶

◀

▶

Back

Close

Full Screen / Esc

Print Version

Interactive Discussion

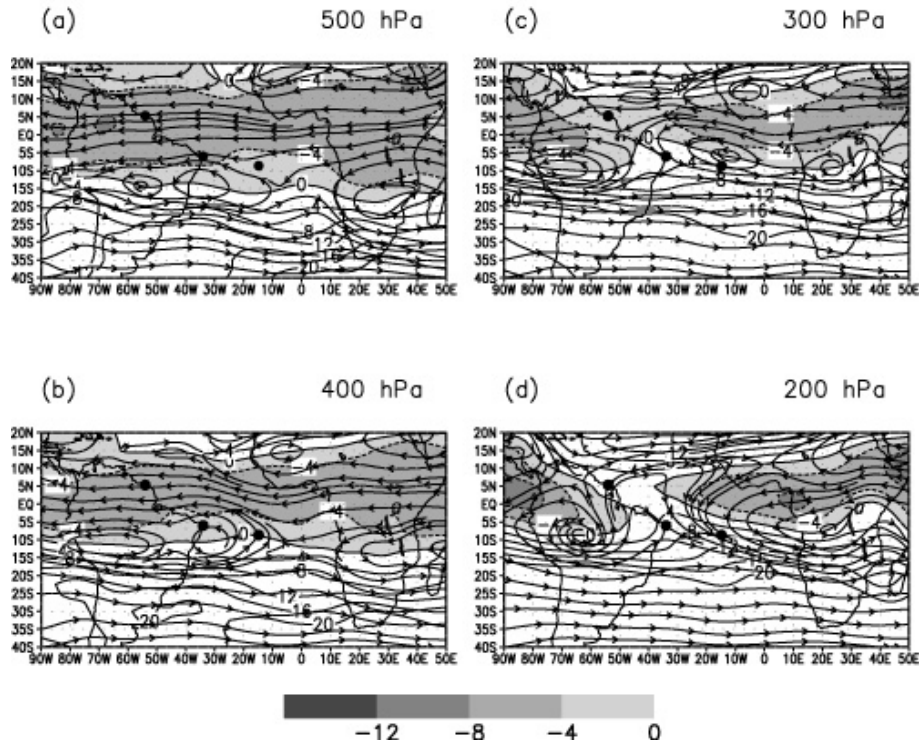
© EGU 2003

## Streamline (arrow) and zonal wind (contour)

1998–2001

September–October–November

September–October–November



**Fig. 13.** 1998–2001 SON middle/upper troposphere zonal winds and streamlines for (a) 500 hPa, (b) 400 hPa, (c) 300 hPa, (d) 200 hPa. Shaded regions are easterly winds. Units are  $\text{m}\cdot\text{s}^{-1}$ .

---

**Space-borne  
observations link**

G. S. Jenkins and  
J.-H. Ryu

---

[Title Page](#)
[Abstract](#)
[Introduction](#)
[Conclusions](#)
[References](#)
[Tables](#)
[Figures](#)
[◀](#)
[▶](#)
[◀](#)
[▶](#)
[Back](#)
[Close](#)
[Full Screen / Esc](#)
[Print Version](#)
[Interactive Discussion](#)

© EGU 2003